

A NUMERICAL STUDY OF BALLISTIC BEHAVIOUR OF CERAMIC METALLIC BI-LAYER ARMOR UNDER IMPACT LOAD

M.K. Khan¹, M.A. Iqbal^{1*}, V. Bratov², N.K. Gupta³, N.F. Morozov²

¹Department of Civil Engineering, Indian Institute of Technology Roorkee, Roorkee-247667, India

²Institute for problems in Mechanical Engineering of the Russian Academy of Sciences, Saint Petersburg State University, St. Petersburg, Russia

³Department of Applied Mechanics, Indian Institute of Technology Delhi, New Delhi-110016, India

*e-mail: iqbal_ashraf@rediffmail.com

Abstract. A 3D finite element model has been developed for studying the ballistic behaviour of bi-layer ceramic-metal target plates under the impact loads induced by the projectiles of different diameter to length ratios. The bi-layer target constituted of alumina 95, as front layer, backed by aluminium alloy 2024-T3 layer, has been impacted by steel 4340 blunt and ogival nosed projectiles of diameter to length ratios, 0.5 and 1.1. The constitutive behaviour of ceramic was modelled using the Johnson-Holmquist (JH-2) constitutive model while that of the metallic backing and the projectile using the Johnson-Cook (JC) material model. The range of incident velocity of the projectile was considered between 800-1000 m/s. The residual projectile velocity, damage induced in the target as well as the projectile, and the ballistic limit velocity (BLV) have been obtained for the different diameter to length ratios (of projectile).

Keywords: ballistic resistance, ceramic-metal armor, residual velocity, finite element modelling

1. Introduction

The advanced ceramic based composite armor has replaced the traditional metallic armor on a large scale, due to some specific material characteristics such as high compressive strength, high hardness and low density. The bi-layer composite armor due to superior ballistic properties and light weight in comparison to the traditional monolithic metallic armor is a most suitable alternative for an effective armor. The function of ceramic layer is to shatter and blunt the projectile, however, during this process, the ceramic is also fractured. The ceramic with no backing will be inadequate to withstand the ballistic impact, as it will break instantaneously due to very little fracture toughness it possesses. The inherent low fracture toughness and less tensile strength of ceramic is a crucial part of the design as these properties are critically important for the desired functioning of an armor. The metallic plates or composite layers are used as backing layer to the ceramic for imparting ductility and tensile strength to the protective system. The backing layer also serves the purpose of keeping the ceramic in its place after the comminution under the impact load and absorbing the remaining kinetic energy of the projectile by undergoing plastic deformation.

A bi-layer ceramic composite armor can resist a particular level of threat at considerably lower weight than a monolithic metal armor. During the penetration of the projectile into a ceramic bi-layer armor, a negligible proportion of the projectile's kinetic energy (0.2 %)

dissipates into fracture of the ceramic. The major energy dissipating mechanisms were identified as plastic deformation of both the backing plate (20-40 %) and the penetrator (10-15 %), and the kinetic energy picked up by the ceramic debris (45-70 %) [1].

During a high velocity impact, a compressive shock wave travels from the impact point on the striking surface to the rear surface, through the thickness of the target, which results in the formation of radial cracks just ahead of the projectile head. A tensile wave is reflected back from the interface between front layer and back layer leading to the formation of circumferential cracks at the rear face, and formation of ceramic conoid. The projectile pushes the comminuted ceramic which is restrained by the backing plate, causing the backing plate to bulge outside, providing space for the comminuted ceramic to move. A new fracture conoid with smaller diameter is formed and segregated from the adjoining material and the procedure kept on repeating until the diameter of the conoid becomes equivalent to that of the diameter of the deformed projectile. The backing plate reaches its strength and the plugs are ejected from the metallic plates with a diameter equivalent to that of the diameter of the deformed projectile [2]. The high velocity impact on a bi-layer target is a complex process which is governed by many factors. The thickness of the plates, constraint conditions, angle of impact and properties of the material are few important factors that affect the failure mechanics involved.

The researchers in the past have studied various factors and conditions affecting the ballistic properties in case of bi-layer ceramic-metal armor. The model given by Florence [3] was one of the early stage study of the ballistic behaviour of ceramic. The model assumed a short cylindrical rod striking normally into the ceramic, forcing it to break progressively into a cone of fractured material, which distributes all the impact energy to the backing plate over a larger area than the projectile's diameter. The backing plate would deform as a uniform membrane under constant tension. As the energy dissipated in ceramic fracture and projectile erosion was ignored, the failure mechanisms of the backing plate was simplified significantly. Based on these assumptions, Florence managed to obtain a fairly simple expression for the ballistic limit for two-component armor. Woodward [1] developed a simple set of models for the perforation of ceramic composite armor, illustrating the relation and effects of various physical properties and impact parameters on the ballistic resistance of the armor. Various aspects such as inertial response of the system components, cone crack formation and projectile erosion and backing deformation were modelled realistically. Hetherington [4] developed an equation for optimum thickness ratio of ceramic to metallic back layer to provide a specified level of protection at minimum weight. The model was developed under a given aerial density with the total thickness of the armor not being constant. The experimental trials with 7.62 AP ammunition against alumina/aluminium combinations confirmed the usefulness of the model. Hetherington observed that for a given areal density, better performance can be obtained with ratios of ceramic to the backing plate as one, or more than one, and that the ratios of less than one can lead to significantly reduced performance. For a normal impact on ceramic target with thin metallic backing plate, a model was proposed by Cortes et al. [5]. The model was based on finite difference lagrangian formulation. There was no front confinement and the penetrator considered was made up of steel. The target was constituted of alumina front plate and aluminium backing plate. The macroscopic material behaviour in the zone of finely pulverized ceramic ahead of the penetrator was modelled by means of a constitutive relation taking into account internal friction and volumetric expansion. When the ceramic was pulverized in front of projectile head, the projectile started pushing it rather than penetration. Woodward et al. [6] performed ballistic experiments on alumina, titanium diboride, toughened zirconia and soda lime glass using tungsten alloy projectile. They concluded that ballistic performance of ceramic may be influenced by the nature and thickness of the ceramic, the confining and backing layers and the geometry of the impacting

projectile. Wang et al. [7] performed experiments to observe the dynamic response of a bi-layer ceramic-metal armor. The bi-layer target was constituted of alumina of 94% purity backed by aluminium alloy 6061 T6. The projectile used in the study was NATO 7.62 AP, 0.5 (12.7 mm) calibre. The experimental data was used to develop an empirical equation for kinetic energy required for complete perforation of the armor. Zaera and Galvez [8] presented a new analytical model for simulation of normal and oblique impact problem in case of bi-layer ceramic-metal armor. The model was based on Tate and Alekseevskii's equation for projectile penetration and on the ideas of Woodward's and den Reijer's models for metallic backing and was validated by comparing experimental and analytical results. Lee and Yoo [9] carried out experiments and numerical simulation to find optimum ratio of thicknesses of ceramic and backing plate in bi-layer armor as it could also affect the penetration process. The experimental works involved ballistic limit velocity determination of different thickness ratios and the results were used for verification of numerical approach. The armor was constituted of alumina ceramic (3380 kg/m^3) front plate and 5083 aluminium backing plate and the projectile used was made up of steel (7850 kg/m^3). The Mohr Coulomb (MC) strength model and linear equation of state (EOS) were used for the simulation performed in AUTODYN hydrocode by using SPH (Smoothed particle hydrodynamics). Chi et al. [2] developed a semi-analytic ballistic limit velocity model based on a numerical study. Using the numerical simulation model they concluded that for a particular bi-layer armor under same geometric ratios the residual velocity remains same. Serjouei et al. [10] validated numerical simulation model by using the data of experiments they performed. The numerical simulation model was then used for validating the model proposed by Chi et al. [2]. The numerical simulation model was used for finding optimum thickness ratios of ceramic and metal plates. Venkatesan et al. [11] studied the behaviour of different aluminum alloys backing plate against ogive nosed projectile by using numerical simulation model. Venkatesan et al. [12] compared the ballistic performance of alumina and silicon carbide ceramic using the numerical simulation and observed that the silicon carbide target performed better in a bi-layer armor.

In the present study, a numerical simulation model has been initially validated by using experimental data of Serjouei et al. [10]. The numerical simulation model was validated by comparing the residual velocity and length of the projectile, and the damage area of the target. The effect of projectile diameter to length ratios has been subsequently studied on the ballistic resistance offered by the bi-layer ceramic metal target, keeping the projectile mass constant. Blunt and ogival nose shaped projectiles have been considered. The ballistic limit velocity was found to be higher in case of the higher diameter to length ratios. The damage induced in the target and the projectile was also discussed.

2. Numerical Simulation

Numerical simulation is very helpful in providing the insight about the behaviour of projectile as well as target during the ballistic penetration if proper modelling is carried out and an appropriate constitutive model has been used. There are many constitutive models available in the literature for predicting the material behaviour of concrete. Nevertheless, the Johnson-Holmquist models are widely used for the material modelling of ceramics under high velocity impact. In the current numerical study, the Johnson and Holmquist 2 (JH-2) [13] model was used for the ceramic and the Johnson-Cook model (JC) [14] for the metallic projectile as well as the backing plate. The parameters taken from Serjouei et al. [10] are presented in Table 1 and 2.

Johnson and Holmquist-2 Model. The normalized equivalent stress is

$$\sigma^* = \sigma_i^* - D(\sigma_i^* - \sigma_f^*), \quad (1)$$

where σ_i^* is the normalized intact equivalent stress, and σ_f^* the normalized fracture stress, and D is the damage ($0 \leq D \leq 1.0$).

The normalized equivalent stresses (σ^* , σ_i^* , σ_f^*) have the general form

$$\sigma^* = \frac{\sigma}{\sigma_{HEL}}, \quad (2)$$

where σ is the actual equivalent stress and σ_{HEL} is the equivalent stress at the Hugoniot elastic limit (HEL). The HEL is the net compressive stress corresponding to the uniaxial strain (shock wave) exceeding the elastic limit of the material. The HEL contains both the pressure and deviator stress components [13].

The normalized intact strength is given by:

$$\sigma_i^* = A(P^* + T^*)^N(1 + C \ln \varepsilon^*) \quad (3)$$

and the normalized fracture strength is given by:

$$\sigma_f^* = B(P^*)^M(1 + C \ln \varepsilon^*). \quad (4)$$

The material constants are A , B , C , M , N , and SFMAX. The SFMAX is the normalized maximum fractured strength, which is included in computation for limiting the normalized fracture strength.

The normalized pressure is:

$$P^* = \frac{P}{P_{HEL}}, \quad (5)$$

where P is the actual pressure and P_{HEL} is the pressure at the HEL. The normalized maximum tensile hydrostatic pressure is:

$$T^* = \frac{T}{P_{HEL}}, \quad (6)$$

where T is the maximum tensile hydrostatic pressure the material can withstand. The dimensionless strain rate is:

$$\varepsilon^* = \frac{\dot{\varepsilon}}{\dot{\varepsilon}_0}, \quad (7)$$

where $\dot{\varepsilon}$ is the actual strain rate and $\dot{\varepsilon}_0 = 1.0 \text{ s}^{-1}$ is the reference strain rate. The damage for fracture is accumulated in a manner similar to that used in the JH-1 model and the Johnson-Cook fracture model. It is expressed as:

$$D = \sum \frac{\Delta \varepsilon_p}{\varepsilon_p^f}, \quad (8)$$

where $\Delta \varepsilon_p$ is the plastic strain during a cycle of integration and $\varepsilon_p^f = f(P)$ is the plastic strain to fracture under a constant pressure, P . The specific expression is:

$$\varepsilon_p^f = D_1(P^* + T^*)^{D_2}, \quad (9)$$

where D_1 and D_2 are constants. The hydrostatic pressure before fracture begins ($D = 0$) is simply:

$$P = K_1\mu + K_2\mu^2 + K_3\mu^3, \quad (10)$$

where K_1 , K_2 and K_3 are constants (K_1 is the bulk modulus); and

$$\mu = \frac{\rho}{\rho_0} - 1. \quad (11)$$

For current density ρ and initial density ρ_0 . After damage begins to accumulate ($D > 0$), bulking (pressure increase and/or volumetric strain increase) can occur. Bulking is related to the change in the volume under the effect of hydrostatic pressure. When damage begins to accumulate, some change in the volume can occur. Now, an additional incremental pressure, ΔP , is added, such that:

$$P = K_1\mu + K_2\mu^2 + K_3\mu^3 + \Delta P. \quad (12)$$

The correct evaluation of JH-2 parameters for a material is not an easy task, as some of the parameters cannot be determined explicitly. The basic ultrasonic technique is generally used for determining the elastic constants of the ceramic. The K_1 , K_2 and K_3 in the pressure-

volume relationship is determined by third degree polynomial fitting on the data of quasi-static pressure-volume response of the material up to high pressures. The data of pressure-volume response of ceramic at very higher pressure can be obtained by diamond-anvil test. The planar plate impact test is used for determination of HEL. The other strength and damage model constants are worked out by best fit to match the computational and experimental data. The split Hopkinson pressure bar test is used for calibrating the strain rate material constant. The procedure of determining the constants was discussed in detail by Holmquist et al. in [15].

Table 1. Parameters for Alumina 95% [10]

| S. No. | Parameters | Values |
|--------|---|------------|
| 1 | Density(Kg/m ³) | 3741 |
| 2 | EOS | Polynomial |
| 3 | Bulk Modulus K_1 (GPa) | 184.56 |
| 4 | Pressure Constant, K_2 (GPa) | 185.87 |
| 5 | Pressure Constant, K_3 (GPa) | 157.54 |
| 6 | Strength Model | JH-2 |
| 7 | Shear Modulus G (GPa) | 120.34 |
| 8 | Hugoniot,elastic limit (HEL) (GPa) | 6 |
| 9 | Intact strength constant, A | 0.889 |
| 10 | Intact strength exponent, N | 0.764 |
| 11 | Strain rate constant, C | 0.0045 |
| 12 | Fracture strength constant, B | 0.29 |
| 13 | Fracture strength exponent, M | 0.53 |
| 14 | Normalized maximum fractured strength | 1 |
| 15 | Failure model | JH-2 |
| 16 | Normalized hydrostatic tensile limit, T^* (GPa) | -0.3 |
| 17 | Damage constant, d_1 | 0.005 |
| 18 | Damage constant, d_2 | 1 |
| 19 | Bulking factor, β | 1 |

Johnson-Cook Model. The Johnson-Cook (JC) constitutive model describes the strength of engineering alloys at large strains, high strain rates and high temperatures. The flow stress is expressed as an explicit function of strain, strain rate and temperature as follows [14].

The equivalent stress of the model is defined as:

$$\sigma_0 = [A + B(\bar{\epsilon}^{pl})^n] \left[1 + C \ln \left(\frac{\dot{\bar{\epsilon}}^{pl}}{\dot{\epsilon}_0} \right) \right] [1 - \hat{T}^m], \quad (12)$$

where $\bar{\epsilon}^{pl}$ is equivalent plastic strain, and A, B, n and m are material parameters measured at or below the transition temperature T_0 .

The non-dimensional temperature \hat{T} is defined as:

$$\hat{T} = \begin{cases} 0 & \text{for } T < T_0 \\ \frac{T - T_0}{T_0 - T_{melt}} & \text{for } T_0 \leq T \leq T_{melt} \\ 1 & \text{for } T > T_{melt} \end{cases}, \quad (13)$$

where T is the current temperature, T_{melt} is the melting point temperature and T_0 is the transition temperature defined as the one at or below which there is no temperature dependence on the expression of the yield stress.

When $T > T_{melt}$ the material melts down and behaves like a fluid and hence does not offer shear resistance. The temperature effects are not considered in the present study as the temperature considered is not high enough to cause any influence on the material behaviour. The parameters of the Johnson and Cook model are determined by various experiments discussed in details by Iqbal et al. [16].

Serjouei et al. [10] used the projectile of nominal diameter, 7.56 mm, and a nominal length, 30.54 mm. The bi-layer target was constituted of ceramic front plate of size 100 mm \times 100 mm and the metallic back layer of size, 160 mm \times 160 mm. The materials of projectile, front layer and back layer of target were hardened steel 4340, alumina 95% and aluminium alloy 2024-T3, respectively.

Table 2. Parameters for Aluminium and Steel [10]

| S. No. | Parameters | Al-2024-T3 | Steel 4340 |
|--------|------------------------------------|------------|------------|
| 1 | Density(Kg/m ³) | 2785 | 7770 |
| 2 | EOS | Shock | Linear |
| 3 | Bulk Modulus K_1 (GPa) | | 159 |
| 4 | Gruneisen constant | 2 | |
| 5 | Parameter C1 (m/s) | 5328 | |
| 6 | Parameter S1 | 1.338 | |
| 7 | Specific heat, Cr (J/kg.K) | 874.9 | 477 |
| 8 | Strength Model | JC | JC |
| 9 | Shear Modulus, G (GPa) | 26.92 | 77 |
| 10 | Static yield strength, A (GPa) | 0.167 | 0.950 |
| 11 | Strain hardening constant, B (GPa) | 0.596 | 0.725 |
| 12 | Strain hardening exponent, n | 0.551 | 0.375 |
| 13 | Strain rate constant | 0.001 | 0.015 |
| 14 | Thermal softening exponent, m | 0.859 | 0.625 |
| 15 | Melting temperature, (K) | 893 | 1793 |
| 16 | Reference strain rate | 1 | 1 |
| 17 | Failure model | JC | JC |
| 18 | Damage constant, d_1 | 0.112 | -0.8 |
| 19 | Damage constant, d_2 | 0.123 | 2.1 |
| 20 | Damage constant, d_3 | 1.5 | -0.5 |
| 21 | Damage constant, d_4 | 0.007 | 0.002 |
| 22 | Damage constant, d_5 | 0 | 0.61 |

In the present study, a three dimensional finite element model of the bi-layer armor and projectile was made in ABAQUS/CAE. The projectile and target plates both were modelled as deformable bodies with lagrangian elements. The four peripheral boundaries of the target was given fixed condition by restraining against all degrees of freedom. The size taken for both the plates were 150 mm \times 150 mm, with 6 mm thickness. The size of the mesh for target plates was kept constant in all the cases studied i.e.; 0.6 mm in the inner part of 60 mm and increasing gradually towards the peripheral boundaries. The mesh size of 0.6 mm was kept constant for the body of projectile. Eight node brick elements (C3D8R) were considered for

the target plates, see Fig. 1. The meshing was kept similar to the meshing of numerical simulation model reported by Serjouei et al. [10]. The numerical simulation results were found to be in good agreement with the experimental results available in the literature. The developed model was found to be suitable for predicting the failure behaviour of the bi-layer ceramic armor.

3. Results and Discussion

Validation. Serjouei et al. [10] performed experiments with steel 4340 projectiles on alumina 95 tiles of span 100×100 mm and thicknesses 6.04-9.08 mm. The blunt nose projectile of nominal diameter, 7.56 mm, and nominal length, 30.54 mm, was fired with the help of a two stage gas gun. The ceramic front layer was adhered to the aluminium alloy 2024-T3 backing plates of 160×160 mm planar dimension. The thickness of the backing plates was varied between 4.07 mm to 8.25 mm. The flash X-ray system was used to capture the impact event. The impact velocity, residual velocity and residual length of the projectile, and the dimension of the plug ejected out of target after perforation were measured and reported. During the experiments, a nominal obliquity of the projectile was experienced and the impact was not perfectly normal to the target surface. The yaw angle was duly considered in the numerical simulation model developed in the present study, as shown in Fig. 1.

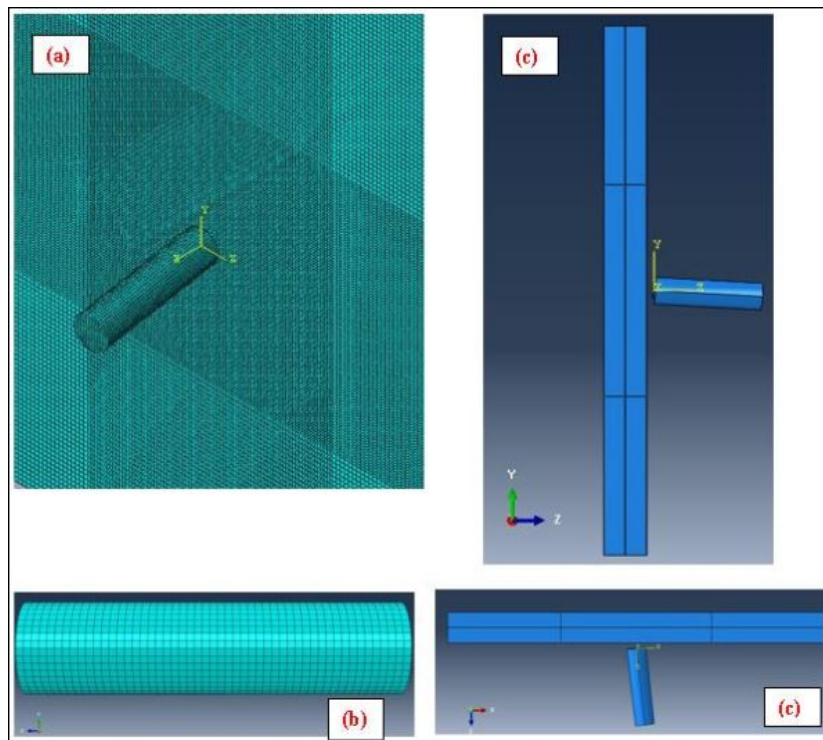


Fig. 1. (a) The meshing of target and projectile (b) The meshing of projectile (c) The presence of yaw angle

A comparison was made for the experimental and computationally obtained residual projectile velocity and residual length of the projectile. After perforation of the target plates, the plug that came out of the plates was measured in two mutually perpendicular directions namely, a_1 and a_2 , see Fig. 2. The numerical simulation model developed in the present study was validated by comparing the residual velocity and length of the projectile and the sizes of the damage zone, a_1 and a_2 . The numerical simulation values of residual velocity and residual length of the projectile, a_1 and a_2 , was found to be very close to the experimental values, as is

reported in Table 3. The numerical simulation model was found to be in good agreement with the experiments and suitable for predicting the failure behaviour of the bi-layer ceramic armor.

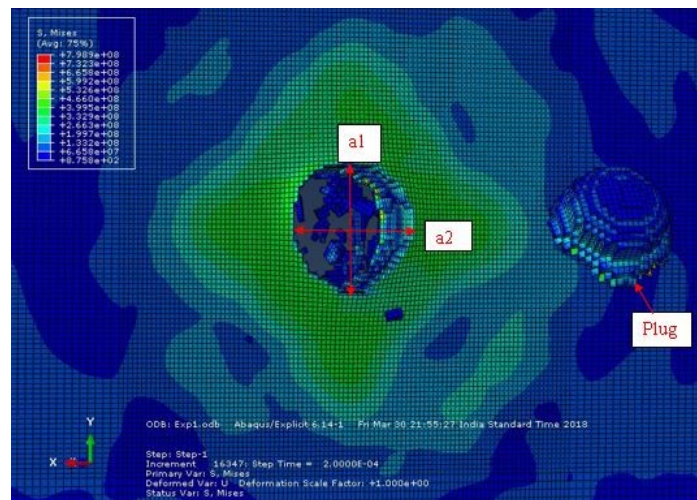


Fig. 2. Damage in terms of size of the hole (a1 and a2) at rear face of backing plate

Table 3. Comparison of experimental data and numerical simulation model

| Parameters | Experiment | Simulation | % Error |
|-------------------|------------|------------|---------|
| Residual Length | 23.4 mm | 25.2 mm | 7.6 |
| Residual Velocity | 351 m/s | 355 m/s | 1.1 |
| a1 | 14 mm | 12.9 mm | 7.8 |
| a2 | 16 mm | 15.1 mm | 5.6 |

Effect of diameter variation. The length to diameter ratio of the projectile was subsequently varied as 0.5 and 1.1 and the simulations were performed at varying incidence velocity for obtaining the ballistic limit of the target corresponding to the two different diameter to length ratios. The diameter of the projectile was considered as 10 and 12.5 mm. The length of projectile was changed accordingly as 17.45 and 11.17 mm to maintain the constant mass of the projectile. Thus, the same mass of the projectile has led to the same kinetic energy and momentum for the different d/l ratios (of projectile). In both the cases of blunt head and ogival nose head, the residual velocity was found to have increased with a decrease in the diameter to length ratio. The comparison of incident velocity to residual velocity is shown for blunt and ogival nosed projectile, respectively, in Fig. 3 and 4. The residual velocity was found to decrease with an increase in the diameter of the projectile. This phenomenon can be attributed to the more interaction zone ahead of the deformed projectile with the comminuted ceramic.

The ballistic limit velocity for the blunt projectiles has been found to have increased with the increase in the diameter to length ratio. The ballistic limit velocities are mentioned in Table 4.

Table 4. BLV for different D/L ratios for blunt projectiles

| S. No. | D/L Ratio | BLV (m/s) |
|--------|-----------|-----------|
| 1 | 0.25 | 435 |
| 2 | 0.5 | 565 |
| 3 | 1.1 | 615 |

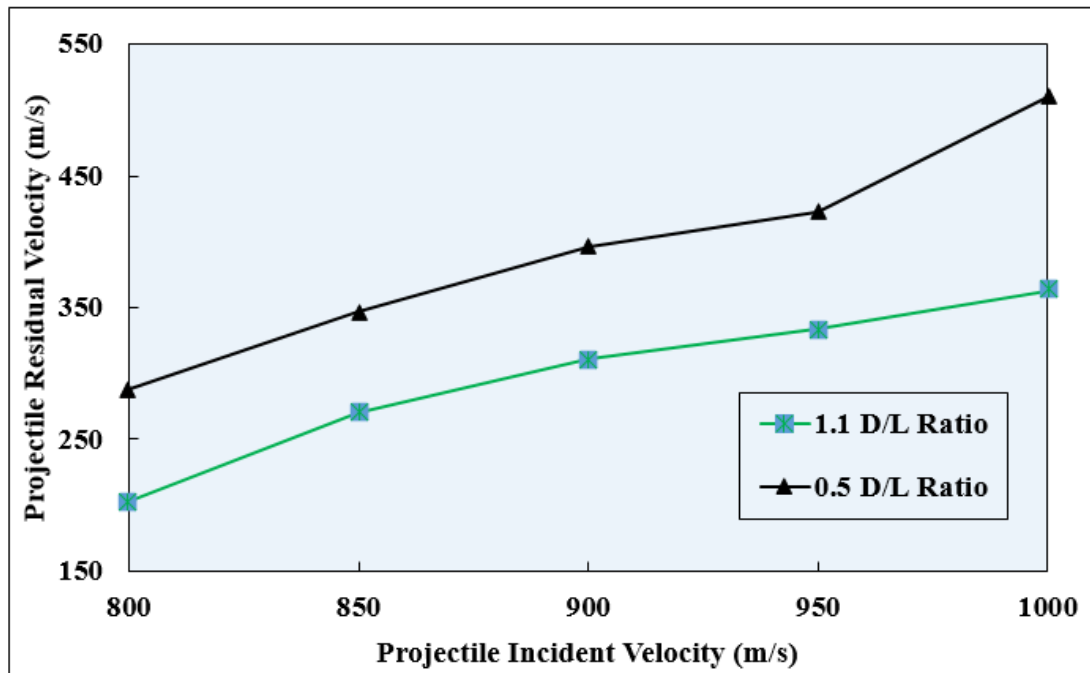


Fig. 3. Variation of Residual velocities with varying impact velocities for different D/L ratios for blunt projectile predicted by developed numerical simulation model

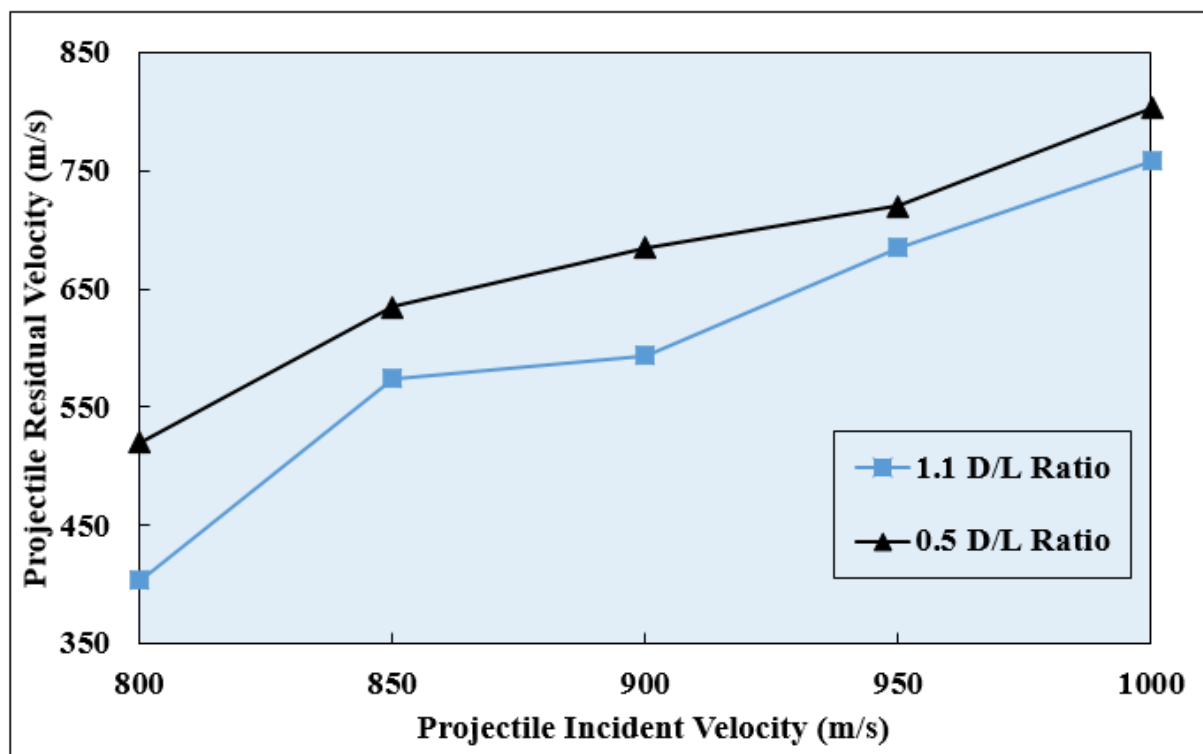


Fig. 4. Variation of Residual velocities with varying impact velocities for different D/L ratios for ogival nosed projectile predicted by developed numerical simulation model

Damage of projectile and bi-layer target. As the bi-layer armor was struck by the projectile, a compressive shock wave was initiated and travelled from the impact point to the interface between ceramic and backing layer. At the interface, this compressive wave was reflected as a tensile wave. The damage in ceramic layer was found to be in two forms; the

compressive failure just ahead of the projectile head which resulted in comminution of ceramic and the tensile failure at the interface of the ceramic-metallic layers which led to the initiation of the circumferential cracks. Fracture conoid was formed with a diameter increasing from ahead of the projectile head to the rear surface. As the projectile further pushed the comminuted ceramic, the backing plate started to bulge and gave space to the comminuted ceramic to move ahead. When the backing plate reached its strength, the projectile perforated the target. The deformation of blunt projectile is shown in Fig. 6. When the ogival nosed projectile hit the target, the tip of the nose fractured. Further damage has occurred to the projectile due to the presence of the comminuted ceramic supported by the backing layer, as shown in Fig. 5.

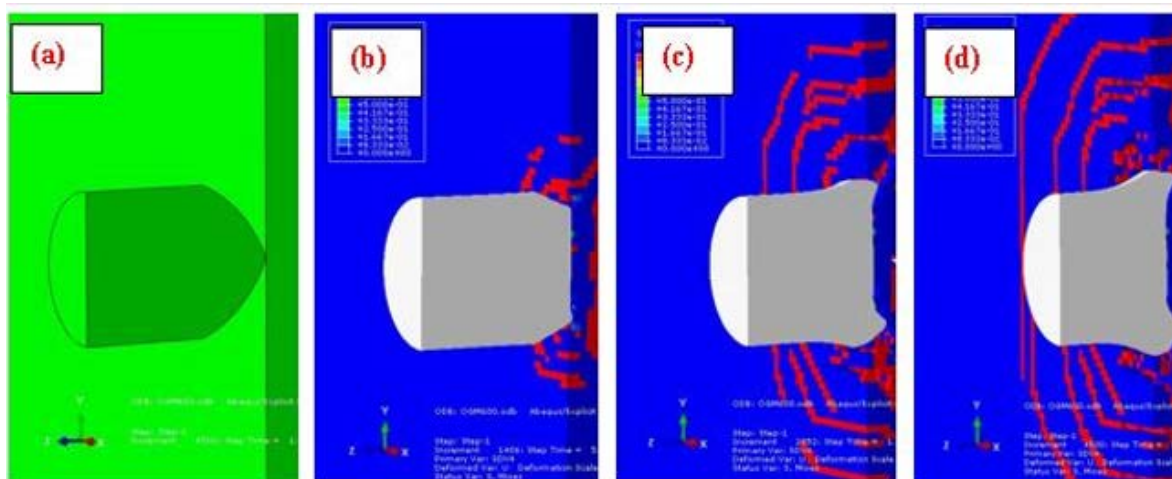


Fig. 5. The deformation of ogival projectile when impacted with a velocity of 600 m/s at (a) 0.0 sec (intact) (b) 5 μ s (c) 10 μ s (d) 15 μ s

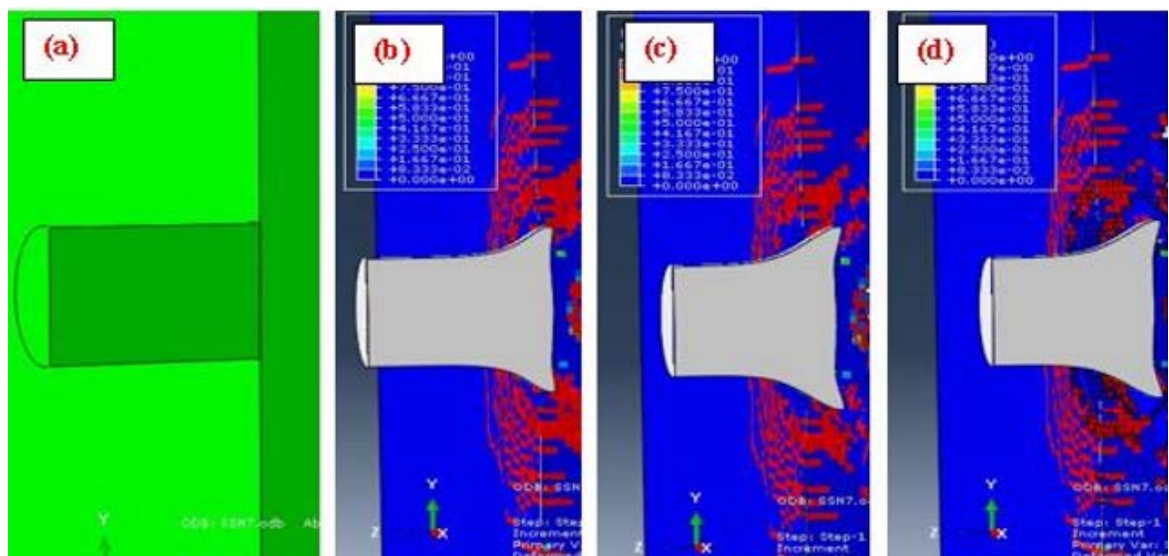


Fig. 6. The deformation of blunt projectile when impacted with a velocity of 610 m/s at (a) 0.0 sec (intact) (b) 8 μ s (c) 16 μ s (d) 24 μ s

The typical damage propagation at rear face of the ceramic layer is shown in Fig. 7 corresponding to the impact velocity 800 m/s. The Fracture conoid in ceramic layer was formed with a diameter of 33 mm for 0.5 D/L ratio and 39 mm for 1.1 D/L ratio of blunt projectiles. The cracks that developed at the ceramic layer were found to be circular with the

diameter of the conoid 33 and 46 mm at the front and rear surface, respectively, against 0.5 D/L ratio. The same has been found to be 39 and 53 mm in the case of 1.1 D/L ratio.

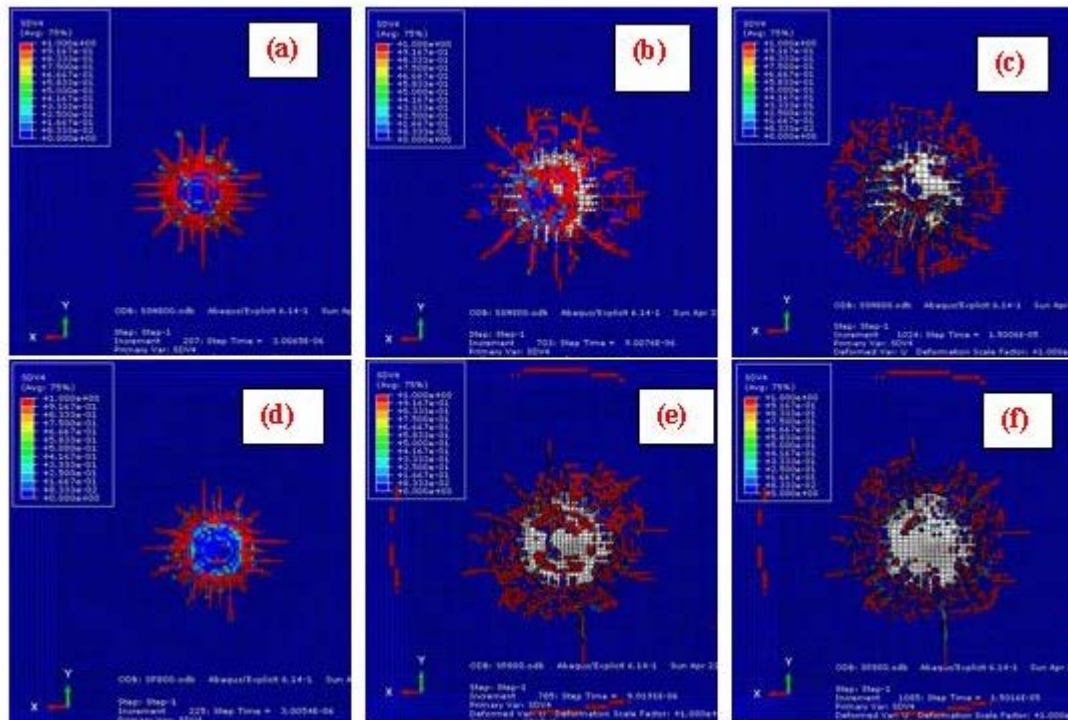


Fig. 7. The damage on rear face of alumina when struck with blunt steel projectile with a velocity of 800 m/s with D/L ratio of 0.5 at (a) 3 μ s (b) 9 μ s (c) 15 μ s and with D/L ratio of 1.1 at (d) 3 μ s (e) 9 μ s (f) 15 μ s

4. Conclusions

A finite element model was developed for studying the impact phenomenon of an incoming projectile on a bi-layer ceramic target. The model was validated by using experimental data available in the open literature. The effect of diameter to length ratios of the projectile on the ballistic behaviour of a bi-layer ceramic-metal target was studied. The mass of the projectile was kept constant to ensure that the projectile approached the target with same kinetic energy and momentum. The residual velocity of the projectile for a particular incident velocity was found to have decreased for higher diameter to the length ratio. The ballistic limit velocity has also been found to be higher with an increase in the projectile diameter to length ratio. This can be attributed to the larger area of interaction ahead of the projectile between the comminuted ceramic and the deformed projectile. The damage induced in the ceramic, metallic plate and the projectile during the penetration process was also studied. The fracture conoid, having smaller diameter on the striking face was observed in the simulation. The diameter of the fracture conoid was found to have increased for the higher diameter to length ratio.

Acknowledgements. Authors gratefully acknowledge the financial support provided by Department of Science and Technology through grant no. INT/RUS/RFBP/P-232 under DST-RFBP scheme for carrying out this research work and financial support provided by the Russian Foundation for Basic Research through grant 19-51-45016 under RFBP-DST scheme.

References

- [1] Woodward RL. A simple one-dimensional approach to modelling ceramic composite armour defeat. *International Journal of Impact Engineering*. 1990;9(4): 455-474.
- [2] Chi R, Serjouei A, Sridhar I, Tan GE. Ballistic impact on bi-layer alumina/aluminium armor: A semi-analytical approach. *International Journal of Impact Engineering*. 2013;52: 37-46.
- [3] Florence AL. *Interaction of Projectiles and Composite Armor. Part II*. California: Standard Research Institute Menlo Park; 1969.
- [4] Hetherington JG. The optimization of two component composite armours. *International journal of impact engineering*. 1992;12(3): 409-414.
- [5] Cortes R, Navarro C, Martinez MA, Rodriguez J, Sanchez-Galvez V. Numerical modelling of normal impact on ceramic composite armours. *International journal of impact engineering*. 1992;12(4): 639-650.
- [6] Woodward RL, Gooch Jr WA, O'donnell RG, Perciballi WJ, Baxter BJ, Pattie SD. A study of fragmentation in the ballistic impact of ceramics. *International Journal of Impact Engineering*. 1994;15(5): 605-618.
- [7] Wang B, Lu G, Lim MK. Experimental and numerical analysis of the response of aluminium oxide tiles to impact loading. *Journal of Materials Processing Technology*. 1995;51(1-4): 321-345.
- [8] Zaera R, Sanchez-Galvez V. Analytical modelling of normal and oblique ballistic impact on ceramic/metal lightweight armours. *International Journal of Impact Engineering*. 1998;21(3): 133-148.
- [9] Lee M, Yoo YH. Analysis of ceramic/metal armour systems. *International Journal of Impact Engineering*. 2001;25(9): 819-829.
- [10] Serjouei A, Chi R, Zhang Z, Sridhar I. Experimental validation of BLV model on bi-layer ceramic-metal armor. *International Journal of Impact Engineering*. 2015;77: 30-41.
- [11] Venkatesan J, Iqbal MA, Gupta NK, Bratov V, Kazarinov N, Morozov NF. Ballistic characteristics of bi-layered armour with various aluminium backing against ogive nose projectile. *Procedia Structural Integrity*. 2017;6: 40-47.
- [12] Venkatesan J, Iqbal MA, Madhu V. Ballistic performance of bilayer alumina/aluminium and silicon carbide/aluminium armours. *Procedia engineering*. 2017;173: 671-678.
- [13] Johnson GR, Holmquist TJ. An improved computational constitutive model for brittle materials. *AIP Conference Proceedings*. 1994;309(1): 981-984.
- [14] Johnson GR. A constitutive model and data for materials subjected to large strains, high strain rates, and high temperatures. In: *Proc. 7th Inf. Sympo. Ballistics*. 1983. p.541-547.
- [15] Holmquist TJ, Templeton DW, Bishnoi KD. Constitutive modeling of aluminum nitride for large strain, high-strain rate, and high-pressure applications. *International Journal of Impact Engineering*. 2001;25(3): 211-231.
- [16] Iqbal MA, Senthil K, Bhargava P, Gupta NK. The characterization and ballistic evaluation of mild steel. *International Journal of Impact Engineering*. 2015;78: 98-113.